RADAR DATA CUBE ANALYSIS FOR FALL DETECTION

Baris Erol and Moeness G. Amin

Center for Advanced Communications, Villanova University, Villanova, PA, 19085, USA

ABSTRACT

In recent years, radar has been employed as a fall detector, due to its superior sensing capabilities and penetration through walls. In this paper, we introduce a multi-linear subspace fall detection scheme that exploits the three radar signal variables: slow-time, fast-time, and Doppler frequency. The proposed approach attempts to find the optimum orthonormal subspaces that minimize the reconstruction error for different modes of the radar data cube. Experimental results based on real radar data obtained from multiple subjects and aspect angles demonstrate that the proposed multi-dimensional principal component analysis (MPCA) yields the highest overall classification accuracy among other methods including physically interpretable pre-defined features and spectrogram-based standard PCA.

Index Terms— Fall detection, principle component analysis, multi-linear subspace learning

1. INTRODUCTION

Falls are the major cause of accidents in the elderly population [1]. Recent studies have revealed that falls were the leading cause of fatal and non-fatal injuries for people aged 65 and over. Therefore, fall detection systems have been identified as a major innovation opportunity to improve the quality of elderly life. Much attention has been recently given to fall detection using radio frequency (RF) sensing modality. This rising interest is driven by advances in machine learning, hardware-software integration, and an aging population requiring effective elderly care and assisted living [2–5]. Different contributions to fall detection have proposed different features that include pre-defined and automatically learned. Whereas most work has focused on pre-defined physically interpreted features [6–8], recent classification efforts have applied deep learning [9–12]. The latter lacks the availability of large data size for proper training and performance validations. In addition to the approaches based on pre-defined and learned features, motion classifications using standard principal component analysis (PCA) has proven effective and provided promising fall classification rates [13, 14]. PCA has been applied to different data representation domains and used to determine suitability of each domain for motion discrimination [15]. In this paper, we apply PCA to the radar data cube (RDC), rather than lower-dimension processing.

Radar backscattering signals from range-Doppler radar, like frequency modulated continuous wave (FMCW), provide target information along the three variables of fast-time, slow-time, and Doppler frequency. Accordingly, two-dimension (2D) joint-variable signal representations can be constructed, depicting the received data in the time-frequency (TF) domain, the range-Doppler (RD) domain, and the range vs. slow-time (range-map) domain. Compared to one-dimension (1D) single-variable domain, the 2D joint-variable representations have shown to reveal intricate properties of the target complex motions, specifically the time-dependency of target velocity, acceleration and higher-order motion moments. Each 2D motion data representation provides distinct and valuable information that might not be present in other 2D domains.

This paper marks the first attempt to use three-dimension (3D) joint-variable signal representation to exploit the underlying dependency and correlations among the three radar signal variables. Encouraged by the classification results of standard PCA, and recognizing possibilities for improvements, we pursue multi-dimensional PCA (MPCA) using tensor analysis [16, 17]. Moreover, an unsupervised multi-linear feature extraction method for RDC is introduced. It is shown that the proposed method outperforms both standard PCA and the case pre-selected features.

The paper is organized as follows. In Section 2, the tri-domain representations of radar signals are presented. In Section 3, the extraction process of pre-defined physically interpreted features is described in detail. In Section 4, proposed MPCA and standard PCA are explained in detail with pre-processing step. In Section 5, the performance of the proposed MPCA is contrasted with pre-defined features and standard PCA. Finally, in Section 6, key conclusions are presented.

2. TRI-DOMAIN REPRESENTATION OF RADAR SIGNALS

Range-map data representation depicts the change in target's range information over time. An example of range map is depicted in Figure 1-(a) for falling. The second domain is referred to as the TF domain and has been extensively employed to represent radar backscattering signals from human

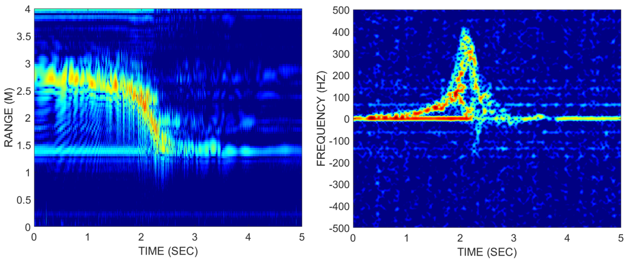

(a) Range-map (b) TF domain

Fig. 1: 2D joint-variable representations of falling data

subjects [18]. In this work, we use the spectrograms, which is the magnitude square of the short time Fourier transform (STFT), to represent raw Doppler signals in the TF domain. The spectrogram of a discrete signal $s(n)$, $n = 0, 1, ..., N-1$ is defined as:

$$\mathrm{S}(n,k) = \left| \sum_{m=0}^{N-1} \mathrm{s}(n+m)\mathrm{h}(m)e^{-j2\pi mk/N} \right|^2 \tag{1}$$

where $h(m)$ is a window function that has an effect on both time and frequency resolutions. In the examples included in this paper, spectrograms are generated using 1024 frequency samples, a Hanning window of length 512, and an overlap of 256 samples. Signal power concentrations in the TF domain are also referred as micro-Doppler signatures [19]. An example of micro-Doppler signature for falling is shown in Figure 1-(b).

RD representation includes the effects of both target velocity and range. Typically, a single RD frame can be obtained by applying the Fourier transform for each range bin over a period of slow-time. The multi-dimensional tensor structure, created by stacking consecutive RD frames, is called RDC. Visualization of the RDC is usually done by a video sequence of RD frames, however, in [20], RDC is visualized by creating a surface that has the same intensity value within the slices of data cube. This can be accomplished by isosurface method which is a 3D extension of an analog isoline. Volumetric representations of the RDC for falling, sitting, bending, and walking are presented in Figure 2-(a), (b), (c), and (d) respectively. Note that, RDC gathers fast-time, slow-time, and Doppler frequency information in a single domain which is the motivation behind using RDC to increase detection and reduction of false alarms.

3. FEATURE EXTRACTION METHODS

A vast number of pre-defined features related to physical characteristics and kinematics of motions has been proposed for human activity recognition with radar. In this work, we consider 3 candidate spectrogram-based features: extreme Doppler frequency, extreme torso frequency, and length of the event. In addition to spectrogram-based features, we also introduce the range spread feature extracted from the range-map. The extreme Doppler frequency is obtained using an energy-based thresholding algorithm. The energy corresponding to the slow time n is computed from the spectrogram as

$$E_T(n) = \sum_{k=1}^{M} \mathrm{S}(n,k)^2 \tag{2}$$

where $k = 1, 2, ..., M$ are the Doppler indices. Next, for each slow-time index n, the first frequency bin whose corresponding spectrogram value is greater than or equal to the product of a pre-determined threshold and E_T is determined as the envelope from which the extreme Doppler frequency can be obtained. The extreme torso frequency, f_{torso}, defined as

$$f_{torso} = \max_n | -1/2T_s + (\lambda_n - 1)/(M-1)T_s| \tag{3}$$

where $\lambda_n = \arg\max_k S(n,k)$ and T_s is the sampling frequency.

4. MULTI-LINEAR SUBSPACE APPROACH FOR FEATURE EXTRACTION

4.1. Multi-linear Algebra Basics and Notations

In this section, we introduce basic concepts that are fundamental to the understanding of the underlying multi-linear subspace methods. Vectors are denoted by lowercase symbols, such as p; the normal uppercase symbols represent matrices, e.g., A. An Nth-order tensor is denoted as $\mathcal{X} \in \mathbb{R}^{I_1 \times I_2 \ldots \times I_N}$. Implemented algorithms often require reshaping of the data, in the case of tensors this operation is called unfolding, or matricization. Unfolding $\mathcal{X}$ along the n-mode is denoted as $\mathcal{X}^{(n)} \in \mathbb{R}^{I_n \times (I_1 \times \ldots \times I_{n-1} \times I_{n+1} \ldots \times I_N)}$. Finally, the n-mode product of a tensor $\mathcal{X}$ by a matrix A is defined by $\mathcal{Y} = \mathcal{X} \times_n$ A.

4.2. Pre-processing (e-CLEAN)

The first step of the proposed method includes a preprocessing of the RDC. Our approach aims to suppress unwanted distortions or noise effects and enhance the natural structural integrity of the data. Therefore, we consider an extended CLEAN (e-CLEAN) algorithm which directly operates on the individual RD frames. The main principle of the original CLEAN algorithm is to find the highest peaks in an image which correspond to a real target location. At the each step of the algorithm, maximum peak is extracted, then a portion of the point spread function centered at that peak is subtracted until some threshold is met [21]. In our approach, the number of points which are needed to be removed are automatically determined prior to extraction of peaks using a simple and efficient histogram-based method. The output of the algorithm is depicted in Figure 3-(b) when a noisy falling RDC data is given in Figure 3-(a).

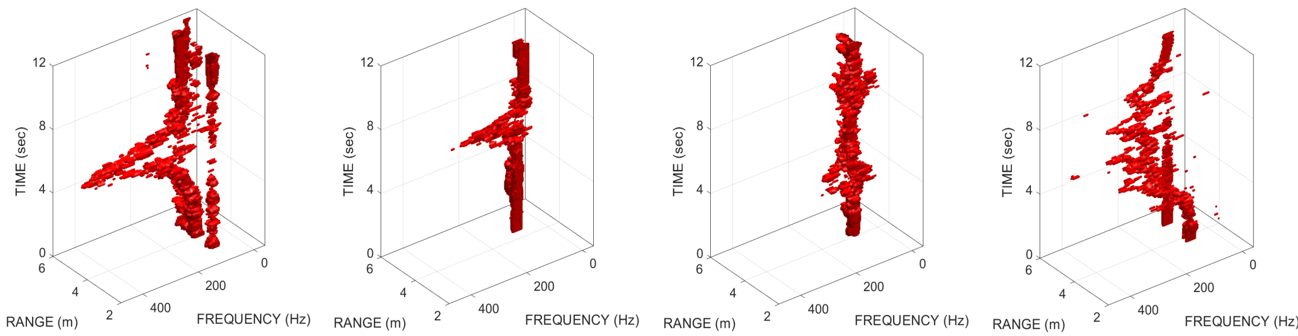

(a) Falling (b) Sitting (c) Bending (d) Walking

Fig. 2: Visualization of the volumetric RDC data for different activities

4.3. MPCA

In order to establish a baseline performance for automated approaches, we first move to consider standard PCA that directly operates on spectrograms. Assume that a set of M training gray-scale spectrograms, $\mathrm{S}_m \in \mathbb{R}^{I_1 \times I_2}$ $m = 1, 2, ..., M$, is vectorized and stored as, $\mathrm{s}_m \in \mathbb{R}^{I_k}$ where $I_k = I_1 \times I_2$. Next, total scatter matrix can be defined as

$$\mathrm{S}_y = \sum_{m=1}^{M} \left(\mathrm{s}_m - \tilde{\mathrm{s}}\right)\left(\mathrm{s}_m - \tilde{\mathrm{s}}\right)^T \tag{4}$$

where the sample mean is defined as, $\tilde{\mathrm{s}} = \frac{1}{M}\sum_{m=1}^{M} \mathrm{s}_m$. The objective of PCA is to maximize the variation captured by the projection samples. The projection matrix U consists of of P projection directions $\{\mathrm{u}_1, \mathrm{u}_2, ..., \mathrm{u}_P\}$. The objective function can then be expressed as

$$\{\tilde{\mathrm{u}}_{(\mathrm{p})}\} = \underset{\mathrm{u}_p;\mathrm{u}_p^T\mathrm{u}_p=1}{\arg\max}\ \mathrm{u}_p^T \mathrm{S}_y \mathrm{u}_p \tag{5}$$

Each projection vector $\tilde{\mathrm{u}}_{(p)}$ can be obtained as the pth eigenvector associated with the pth largest eigenvalue (λ_P) of total scatter matrix. Thus, projection matrix $\tilde{\mathrm{U}}$ contains the eigenvectors corresponding to the P largest eigenvalues of total scatter matrix. These projection matrices are used to train the classifier by projecting the training images into lower dimensions. After classifier is trained, each test sample is projected onto the subspace obtained in the training process.

Next, we introduce an unsupervised multi-linear feature extraction method for RDC. Assume that a set of training tensor samples given as $\mathcal{X}_m \in \mathbb{R}^{I_1 \times I_2 ... \times I_N}$. In the same spirit as goal of standard PCA, our objective is to find a matrix subspace $\tilde{\mathrm{U}}^{(n)} \in \mathbb{R}^{P_n \times I_n}$ that projects the original tensor into a low dimensional tensor subspace $\mathcal{Y}_m \in \mathbb{R}^{P_1 \times P_2 ... \times P_N}$ (with $P_n \leq I_n$). Note that, MPCA scheme generalizes the standard PCA and 2D-PCA algorithms. For $N = 1$, MPCA reduces to standard PCA and for $N = 2$, MPCA is equivalent to the 2D-PCA [16]. We seek to maintain as much as possible variations present in the projected data and minimize the reconstruction error [22]. Original tensor data can be approximated

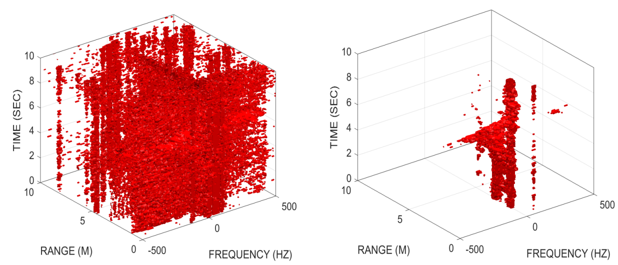

Fig. 3: Visualization of a noisy falling RDC data before and after e-CLEAN

as a multi-linear transformations of a core tensor subspace, $\mathcal{Y}_m$, by the subspace matrices, $\mathrm{U}^{(n)}$, as

$$\tilde{\mathcal{X}}_m \approx \mathcal{Y}_m \times_{(1)} \mathrm{U}^{(1)^T} \times_{(2)} \mathrm{U}^{(2)^T} ... \times_{(N)} \mathrm{U}^{(N)^T} \tag{6}$$

This expression can be defined in an equivalent form as

$$\tilde{\mathcal{X}}_m \approx [\mathcal{Y}_m; \mathrm{U}^{(1)^T}, \mathrm{U}^{(2)^T}, ..., \mathrm{U}^{(N)^T}] \tag{7}$$

Using the same idea of n-mode unfolding and tensor multiplication, the core tensor subspace can be also expressed as

$$\mathcal{Y}_m = [\mathcal{X}_m; \mathrm{U}^{(1)}, \mathrm{U}^{(2)}, ..., \mathrm{U}^{(N)}] \tag{8}$$

To find the best approximation, $\tilde{\mathcal{X}}_m$, provided by the core tensor and subspace matrices, a suitable cost function is required. This can be achieved by minimizing the Frobenius norm, $\|.\|_{\mathrm{F}}$, of the difference between the given data tensor and its approximation defined as

$$\tilde{\mathrm{U}}^{(\mathrm{n})} = \underset{\mathrm{U}^{(n)}}{\arg\min} \sum_{m=1}^{M} \left\|\mathcal{X}_m - [\mathcal{Y}_m; \mathrm{U}^{(1)^T}, \mathrm{U}^{(2)^T}, ..., \mathrm{U}^{(N)^T}]\right\|_{\mathrm{F}}^2$$
$$\text{subject to } \mathrm{U}^{(n)} \times \mathrm{U}^{(n)^T} = \mathrm{I},\ n = 1, 2, ..., N \tag{9}$$

By expanding the Frobenius norm while keeping the subspaces orthonormal, the objective function can be further ex-

Table 1: Pre-defined features (Accuracy: 87.87%)

	Fall	Non-fall
Fall	82.03	17.97
Non-fall	6.29	93.71

Table 2: 17 projection standard PCA (Accuracy: 86.01%)

	Fall	Non-fall
Fall	79.79	20.21
Non-fall	7.76	92.24

Table 3: 5 projection MPCA (Accuracy: 97.88%)

	Fall	Non-fall
Fall	96.62	3.38
Non-fall	0.86	99.14

pressed as

$$\tilde{\mathrm{U}}^{(\mathrm{n})} = \arg\min_{\mathrm{U}^{(n)}} \sum_{m=1}^{M} \|\mathcal{X}_m\|_{\mathrm{F}}^2 - \|\tilde{\mathcal{X}}_m\|_{\mathrm{F}}^2 \tag{10}$$

Since the computation of the approximation is multi-linear, iterative optimization of (10) can be solved through a sequence of linear subproblems using alternating least squares (ALS), whereby the least squares of the cost function is optimized for one mode at a time, while keeping the other mode subspace matrices fixed. Because the cost function is solved using an iterative process, we need an initialization subspace. In this work, the initial subspace matrix, $\mathrm{U}^{(n)^*}$, is constructed randomly, then updated at the each step of the ALS according to the Frobenius norm. Finally, the feature tensor is obtained by projecting the original tensor using optimized subspace, $\tilde{\mathrm{U}}^{(\mathrm{n})}$, as

$$\tilde{\mathcal{Y}}_m = [\mathcal{X}_m; \tilde{\mathrm{U}}^{(1)}, \tilde{\mathrm{U}}^{(2)}, ..., \tilde{\mathrm{U}}^{(N)}] \in \mathbb{R}^{P_1 \times P_2 ... \times P_N} \tag{11}$$

Note that, the dimensionality of the core tensor subspace, P_n, is assumed to be known or predetermined. The effect of the P_n is shown in Section 5 in terms of classification accuracy.

5. EXPERIMENTAL RESULTS

Extensive data measurements were conducted to demonstrate the contribution of the RDC-based MPCA for fall detection. Operating parameters of the ultra-wide band (UWB) radar system that used in the experiments are, transmitting frequency 25 GHz, sampling frequency 1 kHz, and bandwidth of 2 GHz. The dataset contained four human motions: falling (109), sitting (105), bending (95), and walking (76). Each activity was recorded for a duration of 10 seconds, for 6 different subjects and 4 different aspects angles, yielding a total of 385 data samples. Each subject performed each type of motion at 0°, 22.5°, 30°, and 45°. Experiments were collected in Radar Imaging Laboratory at Villanova University.

In the classification stage, a k-Nearest Neighbors (kNN) classifier with $k = 3$ was employed. 70% of the recorded signals were used to train the classifier, whereas the remaining 30% were used as testing. The selection of the training and testing sets were carried out in a randomly fashion. In total 1000 Monte Carlo trials were performed to evaluate the performance of the 3 considered algorithms.

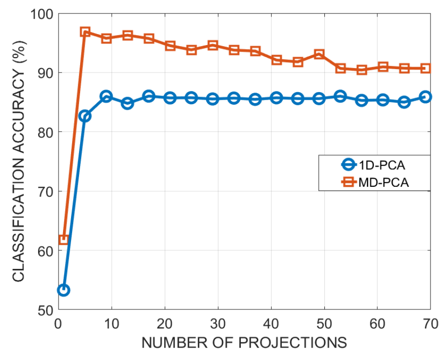

Fig. 4: Dependency of classification accuracy on different number of projections employed in standard PCA and MPCA

Another important question raised in subspace analysis concerns with the number of components (features) needed in the final system. The classification accuracies of standard PCA and MPCA are provided in Figure 4 for different number of projections used. These results clearly show the benefit of this analysis as both algorithms yield their best performance at a relatively small number of features, and do not exhibit much improvements afterwards. The confusion matrices for the three algorithms are provided in Tables 1 through 3. The average classification accuracies for manually extracted pre-defined features, standard PCA, and MPCA are determined to be 87.87%, 86.01%, and 97.88%, respectively. The MPCA produces the lowest number of missed detections and highest fall detection at a rate of 96.62%. In essence, MPCA performance is drastically higher than that achieved with existing commonly used algorithms, proving the importance of RDC.

6. CONCLUSION

In this paper, we proposed a radar data cube (RDC)-based multi-linear subspace method for fall detection. Utilization of RDC offers an effective way to combine motion information from individual domains to capture cross-correlations and inter-dependency. The proposed subspace method benefits from a single representation utilizing the entwined relationship between the fast-time, slow-time, and Doppler frequency and their corresponding joint-variable domains. In employing kNN as the classifier, we demonstrated that, introduced multi-dimensional PCA method outperforms those based on standard PCA and manually extracted features.

7. REFERENCES

[1] E. R. Burns, J. A. Stevens, and R. Lee, "The direct costs of fatal and non-fatal falls among older adults - united states," *Journal of Safety Research*, vol. 58, pp. 99–103, 2016.

[2] M. G. Amin, *Radar for Indoor Monitoring*, CRC Press, 2017.

[3] M. G. Amin, Y. D. Zhang, F. Ahmad, and K. C. Ho, "Radar signal processing for elderly fall detection: The future for in-home monitoring," *IEEE Signal Processing Magazine*, vol. 33, no. 2, pp. 71–80, 2016.

[4] F. Ahmad, A. E. Cetin, K. C. Ho, and J. E. Nelson, "Special section on signal processing for assisted living," *IEEE Sig. Process. Mag.*, vol. 33, no. 2, pp. 25–94, 2016.

[5] O. D. Lara and M. A. Labrador, "A survey on human activity recognition using wearable sensors," *IEEE Communications Surveys & Tutorials*, vol. 15, no. 3, pp. 1192–1209, 2013.

[6] Y. Kim, S. Ha, and J. Kwon, "Human detection using doppler radar based on physical characteristics of targets," *IEEE Geoscience and Remote Sensing Letters*, vol. 12, no. 2, pp. 289–293, 2015.

[7] Q. Wu, Y. D. Zhang, W. Tao, and M. G. Amin, "Radar-based fall detection based on doppler time-frequency signatures for assisted living," *IET Radar, Sonar and Navigation*, vol. 9, no. 2, pp. 164–172, 2015.

[8] B. Y. Su, K. C. Ho, M. J. Rantz, and M. Skubic, "Doppler radar fall activity detection using the wavelet transform," *IEEE Transactions on Biomedical Engineering*, vol. 62, no. 3, pp. 865–875, 2015.

[9] Y. Kim and T. Moon, "Human detection and activity classification based on micro-doppler signatures using deep convolutional neural networks," *IEEE Geoscience and Remote Sensing Letters*, vol. 13, no. 1, pp. 8–12, 2016.

[10] B. Jokanovic, M. G. Amin, and F. Ahmad, "Radar fall motion detection using deep learning," in *2016 IEEE Radar Conference (RadarConf)*, Philadelphia, PA, 2016, pp. 1–6.

[11] M. S. Seyfioglu, S. Z. Gurbuz, A. M. Ozbayoglu, and M. Yuksel, "Deep learning of micro-doppler features for aided and unaided gait recognition," in *2017 IEEE Radar Conference (RadarConf)*, Seattle, WA, 2017, pp. 1125–1130.

[12] B. Jokanovic and M. G. Amin, "Fall detection using deep learning in range-doppler radars," *IEEE Transactions on Aerospace and Electronic Systems*, vol. 54, no. 1, pp. 180–189, 2018.

[13] B. G. Mobasseri and M. G. Amin, "A time-frequency classifier for human gait recognition," *Proc. SPIE*, vol. 73062, 2009.

[14] B. Jokanovic, M. G. Amin, F. Ahmad, and B. Boashash, "Radar fall detection using principal component analysis," *Proceedings of SPIE Radar Sensor Technology XX*, vol. 9829, 2016.

[15] B. Jokanovic and M. G. Amin, "Suitability of data representation domains in expressing human motion radar signals," *IEEE Geoscience and Remote Sensing Letters*, vol. 14, no. 12, pp. 2370–2374, 2017.

[16] H. Lu, K. N. Plataniotis, and A. N. Venetsanopoulos, "Mpca: Multilinear principal component analysis of tensor objects," *IEEE Transactions on Neural Networks*, vol. 19, no. 1, pp. 18–39, 2008.

[17] H. Lu, K. N. Plataniotis, and A. N. Venetsanopoulos, *Multilinear Subspace Learning: Dimensionality Reduction of Multidimensional Data*, Chapman and Hall/Crc, 2012.

[18] V. C. Chen, F. Fi, S. S. Ho, and H. Wechsler, "Micro-doppler effect in radar: phenomenon, model, and simulation study," *IEEE Transactions on Aerospace and Electronic Systems*, vol. 42, no. 1, pp. 2–21, 2006.

[19] V. C. Chen, *The micro-Doppler effect in radar*, Artech House, 2011.

[20] Y. He, P. Molchanov, T. Sakamoto, P. Aubry, F. L. Chevalier, and A. Yarovoy, "Range-doppler surface: a tool to analyse human target in ultra-wideband radar," *IET Radar, Sonar, and Navigation*, vol. 9, no. 9, pp. 1240–1250, 2015.

[21] J. A. Hogbom, "Aperture synthesis with a non-regular distribution of interferometer baselines," *Astronomy and Astrophysics Supplement Series*, vol. 15, pp. 417, 1974.

[22] A. Cichocki, "Tensor decompositions for signal processing applications: From two-way to multiway component analysis," *IEEE Signal Processing Magazine*, vol. 32, no. 2, pp. 145–163, 2015.